Rising methane emissions from northern wetlands associated with sea ice decline

Frans-Jan W. Parmentier[1,2], Wenxin Zhang[1], Yanjiao Mi[3,4], Xudong Zhu[5], Jacobus van Huissteden[3], Daniel J. Hayes[6], Qianlai Zhuang[5], Torben R. Christensen[1,2], and A. David McGuire[7]

[1]Department of Physical Geography and Ecosystem Science, Lund University, Lund, Sweden, [2]Arctic Research Centre, Aarhus University, Aarhus, Denmark, [3]Faculty of Earth and Life Sciences, VU University Amsterdam, Amsterdam, Netherlands, [4]Institute of Arctic Biology, University of Alaska Fairbanks, Fairbanks, Alaska, USA, [5]Department of Earth, Atmospheric, and Planetary Sciences and Department of Agronomy, Purdue University, West Lafayette, Indiana, USA, [6]Environmental Sciences Division, Oak Ridge National Laboratory, Oak Ridge, Tennessee, USA, [7]U.S. Geological Survey, Alaska Cooperative Fish and Wildlife Research Unit, University of Alaska Fairbanks, Fairbanks, Alaska, USA

Abstract The Arctic is rapidly transitioning toward a seasonal sea ice-free state, perhaps one of the most apparent examples of climate change in the world. This dramatic change has numerous consequences, including a large increase in air temperatures, which in turn may affect terrestrial methane emissions. Nonetheless, terrestrial and marine environments are seldom jointly analyzed. By comparing satellite observations of Arctic sea ice concentrations to methane emissions simulated by three process-based biogeochemical models, this study shows that rising wetland methane emissions are associated with sea ice retreat. Our analyses indicate that simulated high-latitude emissions for 2005–2010 were, on average, 1.7 Tg CH_4 yr^{-1} higher compared to 1981–1990 due to a sea ice-induced, autumn-focused, warming. Since these results suggest a continued rise in methane emissions with future sea ice decline, observation programs need to include measurements during the autumn to further investigate the impact of this spatial connection on terrestrial methane emissions.

1. Introduction

Ecosystems in the most northern part of our planet are subject to profound changes, such as an amplified rise in air temperature following the rapid loss of millions of square kilometers in Arctic sea ice [*Lawrence et al.*, 2008; *Serreze and Barry*, 2011; *Screen et al.*, 2012; *Bhatt et al.*, 2014]. This sea ice-induced warming feedback extends from the marine to the terrestrial domain and may consequently increase the emission of the potent greenhouse gas methane from high-latitude wetland soils [*Parmentier et al.*, 2013]. A rise in terrestrial methane emissions may therefore be connected to sea ice changes occurring far off within the Arctic Ocean, as illustrated in Figure 1: when sea ice melts and gives way to open ocean, an immense lowering in albedo occurs, which leads to an increase in the absorption of solar heat [*Pistone et al.*, 2014]. This extra heat is emitted back to the atmosphere, causing higher near-surface air temperatures [*Lawrence et al.*, 2008; *Screen et al.*, 2012]. Sea ice decline is, therefore, one of the major drivers behind polar amplification and ultimately affects greenhouse gas exchange [*Parmentier et al.*, 2013]: a warmer Arctic facilitates an intensified production of methane by microbes in wetland soils, leading to higher emissions. However, the precise magnitude and regional impact of this connection is unclear due to a scarcity of measurements, while cause and effect are obscured due to the temperature sensitivity of both methane production and sea ice loss. This leads to considerable doubt on the existence of this connection: is a link between sea ice decline and terrestrial methane emissions truly present, or are they both responding to the same external driver? And, if identified, is it possible to quantify the magnitude and pinpoint the regional extent of this connection? Answering these questions is not just essential to understand the wider consequences of sea ice decline, but of broader importance to flux observation programs that need to know where and when to perform observations to be able to capture long-term trends in methane emissions [*Christensen*, 2014].

Since past methane flux observations are too thinly spread in time and space to resolve large-scale patterns spanning decades, these issues are arguably best explored with the use of models and/or remote sensing. We compared satellite measurements of sea ice concentration [*Comiso*, 2000] to the modeled exchange of
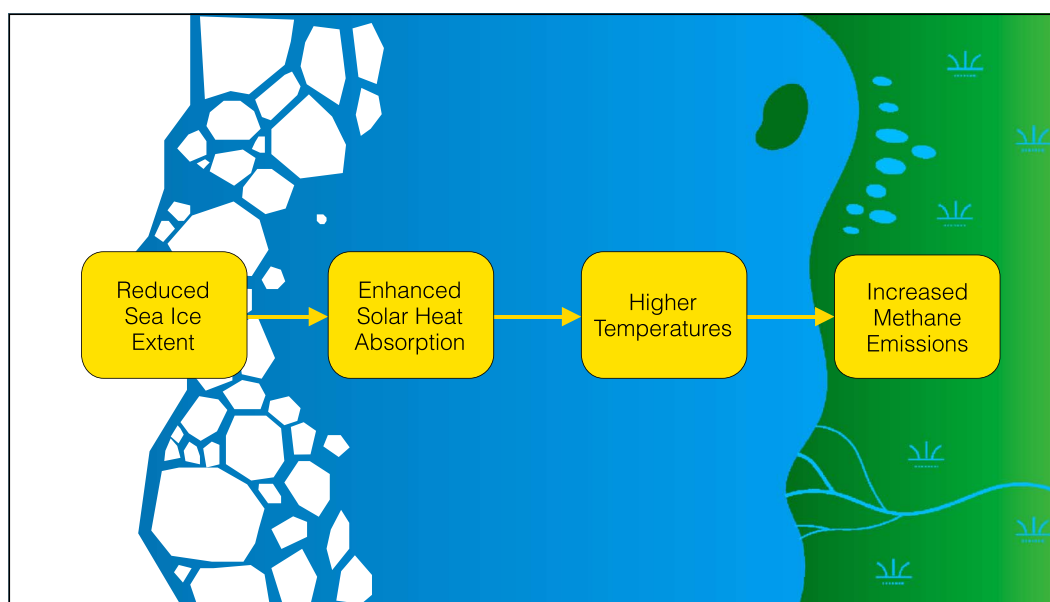
Figure 1. Schematic description of the connection between sea ice decline and increased methane emissions from northern wetlands.

methane from three distinctly different regional process models, LPJ-GUESS [*Smith et al.*, 2001], Peatland-VU [*van Huissteden et al.*, 2006], and TEM6 [*McGuire et al.*, 2010; *Hayes et al.*, 2011], for the area north of 45°N over the 1981–2010 time period. These models vary not only in essential subroutines but also in the climate forcing used as input. The only input that was prescribed identically among the models was wetland fraction, since this leads to large differences between models [*Petrescu et al.*, 2010; *Melton et al.*, 2013]. For further details on model structure and prescribed wetland extent, we refer to the supporting information. If the methane fluxes from all three models show similar correlations to sea ice decline, despite varying approaches, this increases confidence in the realism of the simulated patterns.

2. Methods

2.1. Correlations Between Sea Ice and Methane Emissions

Regional differences are of major importance in this study due to the large spatial variability in both sea ice concentrations and methane emissions: if sea ice retreat occurs close to a region with vast wetlands, it is more likely that methane emissions are affected as opposed to melt occurring far away. Therefore, sea ice concentration was compared to the individual grid cells of the methane models. Around each grid cell, a radius of 2000 km was drawn as an area of interest in which sea ice concentrations were averaged after applying the following distance-weighted function:

$$SIC_{avg} = \frac{\sum_{i=1}^{n} sic_i d_i^{-0.5}}{\sum_{i=1}^{n} d_i^{-0.5}} \qquad (1)$$

SIC_{avg} is the distance-weighted average of sea ice concentration within 2000 km from a model grid cell, sic the sea ice concentration taken from the satellite product [*Comiso*, 2000], and d the distance from the grid cell to each value of sea ice concentration. This grid cell-specific index of sea ice cover represents a weighted average of sea ice concentrations dominated by nearby ice, with less influence from remote sea ice changes. Nonetheless, if large changes in sea ice cover occur at distance, this will still be captured.

To minimize the chance of spurious correlations, both the distance-weighted sea ice concentrations and modeled methane fluxes were linearly detrended over time before correlating. Correlations were set to zero
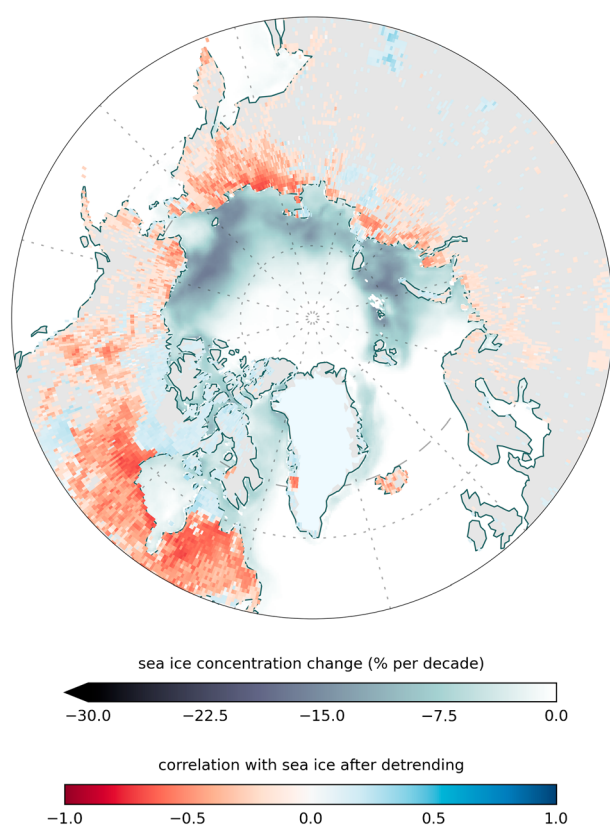
sea ice concentration change (% per decade)

−30.0   −22.5   −15.0   −7.5   0.0

correlation with sea ice after detrending

−1.0   −0.5   0.0   0.5   1.0

Figure 2. Correlations between 1981–2010 May–October terrestrial methane emissions and sea ice concentration. Red to blue colors depict the *r* value of the correlation between modeled methane emissions and sea ice concentration within 2000 km, averaged for all three models. The linear trend in sea ice concentration is shown to indicate areas of high retreat. Note that high correlations do not necessarily equal high emissions.

when they did not achieve the desired significance level ($p > 0.05$). The *r* value of the match between the two time series indicates how well the interannual pattern of methane emissions compares to changes in sea ice extent. Good agreement at this level makes it much more likely that the two are related. Without detrending, a good correlation can be due to a long-term linear trend in both, even when the interannual pattern is unrelated. The latter could in theory be due to many factors, such as an underlying global warming signal [*Najafi et al.*, 2015], instead of regional amplification of methane fluxes indirectly caused by sea ice retreat. Through detrending, we avoid such instances and ensure a conservative approach, since it disregards the long-term warming trend associated with sea ice retreat [*Screen et al.*, 2012].

Influences on the connection between sea ice and methane emissions other than distance, such as dominant wind direction, the albedo of the sea ice, or a lagged response of methane emissions to sea ice decline are not included in this analysis. Positive feedbacks that may enhance Arctic methane emissions, such as permafrost thaw, are also underrepresented. The influence of sea ice onto the climate is implied through information contained within the various climate forcings used, allowing for an independent comparison.

Furthermore, since Peatland-VU runs at a $1 \times 1°$ resolution, each modeled value was split into four new grid cells with the same value to facilitate averaging at the $0.5 \times 0.5°$ resolution of the other models. If a pattern arises from the rudimentary approach outlined above—without modeling the direct influence of sea ice on climatic drivers—this increases confidence that a connection between sea ice and methane emissions exists.

2.2. Comparison of Trends Between Sea Ice-Affected and Unaffected Areas

To extend beyond correlations, it was investigated whether methane emissions increased substantially more in areas influenced by sea ice. The relative increase of the original model output (before detrending) was linearly interpolated against the observed amount of sea ice decline over the period 1991–2010 for each month from spring to autumn. In this case, an ordinary average of sea ice extent was used to allow for equal comparison of the trends from each grid cell with the same independent variable, and subsequent averaging. Trends were calculated as a percentage change relative to the average of methane emissions from 1981 to 1990—a period when sea ice was relatively stable.

After determining trends for each grid cell, they were averaged over two regions: those that correlated well with sea ice decline, and those that did not. Areas with an absolute *r* value larger than 0.3 were considered substantially associated with sea ice decline. Before averaging, all trends separated more than 3 standard deviations from the mean were removed to avoid bias due to extreme outliers, e.g., division with a small number. This filter removed 0.05% to 2.73% of grid cells, depending on the model and month. Lowering this threshold to 2 standard deviations did not affect the results significantly. Arguably, an ordinary sum of fluxes

could have been considered instead of relative changes, but this would lead to a dominance from areas with high emissions—e.g., due to model parameterization or prescribed wetland fraction. Averaging relative trends illustrates the percentage change in methane emissions across the whole area influenced by sea ice, without dominance from such hot spots.

Rather than a change relative to the same fixed amount of sea ice decline for all months (i.e., per 1 million km^2 of sea ice retreat), and to acknowledge the larger decline in the autumn, average trends were multiplied with the absolute difference of the linear trend in monthly sea ice extent between 1991 and 2010. In parallel, the amplified flux of methane specific for the years 2005–2010 was calculated from the average trends by multiplying them with the observed reductions in sea ice retreat and the mean emissions from sea ice-affected areas during the 1981–1990 reference period. The same process was repeated for each climate forcing data set to identify trends in near-surface air temperature for sea ice-affected and unaffected areas. Since temperature changes are less spatially variable than methane emissions, the average change in temperature relative to the 1981–1990 reference period sufficed. The analysis was identical in all other aspects, including the same division in sea ice-affected and unaffected areas.

3. Results

3.1. Spatial and Temporal Correlations With Sea Ice Decline

The correlations between the detrended time series of sea ice and methane are shown in Figure 2 as the average of all three models. A clear negative correlation between May–October methane fluxes and sea ice extent is apparent throughout the Arctic, indicating higher methane emissions in years of lower sea ice extent. The three models agree very well in areas with known wetlands, such as west and northeast Siberia, the north slope of Alaska, and the wetlands surrounding Hudson Bay. Surprisingly, a positive correlation emerged in the Canadian Archipelago and other areas, which implies a decrease in methane emissions concurrent with sea ice decline. This seems contradictory, but the Canadian Archipelago is an area with very few wetlands, and as a result one of the models—TEM6—simulates negative fluxes in this area due to an uptake of methane by dry and aerated soils, a process that is also temperature dependent. These positive correlations suggest an increase in methane oxidation rather than a decrease in methane production. However, the magnitude of the modeled fluxes in these regions is very small (see supporting information Figure S1). These slight changes therefore do not significantly affect the net methane budget of the Arctic in the reverse direction. Overall, Figure 2 shows vast areas within the Arctic where methane emissions covary with the interannual variation of sea ice.

While these correlations are averaged for the May–October period, the contribution of sea ice decline to the amplified surface warming in the Arctic is largest in spring and autumn [*Screen et al.*, 2012], which necessitates a closer examination of this connection throughout the year. Figure 3 shows the average correlations from all three models for each individual month (see supporting information Figure S2 for the month-by-month correlations of each model). In May and June, strong negative correlations appear throughout North America and Eurasia, with especially strong correlations in Canada. This pattern largely disappears during July and August, a time when methane emissions are highest but the influence of sea ice on temperature is rather limited [*Screen et al.*, 2012]. Apart from some parts of northeast Siberia and Alaska, where large areas of sea ice have disappeared, few significant correlations can be found during these months. Areas with good correlations reappear toward the end of the summer, beginning of autumn, especially in Northern Siberia and Alaska. The large decline of sea ice adjacent to these regions raised local air temperatures, and the models indicate that methane emissions have increased accordingly. This pattern of strong correlations with sea ice in spring and autumn corresponds to the warming signature of sea ice retreat [*Screen et al.*, 2012].

Temperature and precipitation are both strong controls on methane emissions, and arguably the most likely environmental factors to be affected by sea ice decline [*Screen et al.*, 2012; *Bintanja and Selten*, 2014]. Therefore, to assess the underlying reason for the emergent patterns shown in Figures 1 and 2, sea ice concentration was compared in precisely the same manner to near-surface air temperature and precipitation of the climate forcing used by each model (see supporting information Figures S3 and S4 for details). From this analysis it appeared that temperature showed a strong similarity to the spatial patterns shown in Figures 1 and 2 (compare Figures S2 and S3 for details), while a connection to precipitation appeared absent
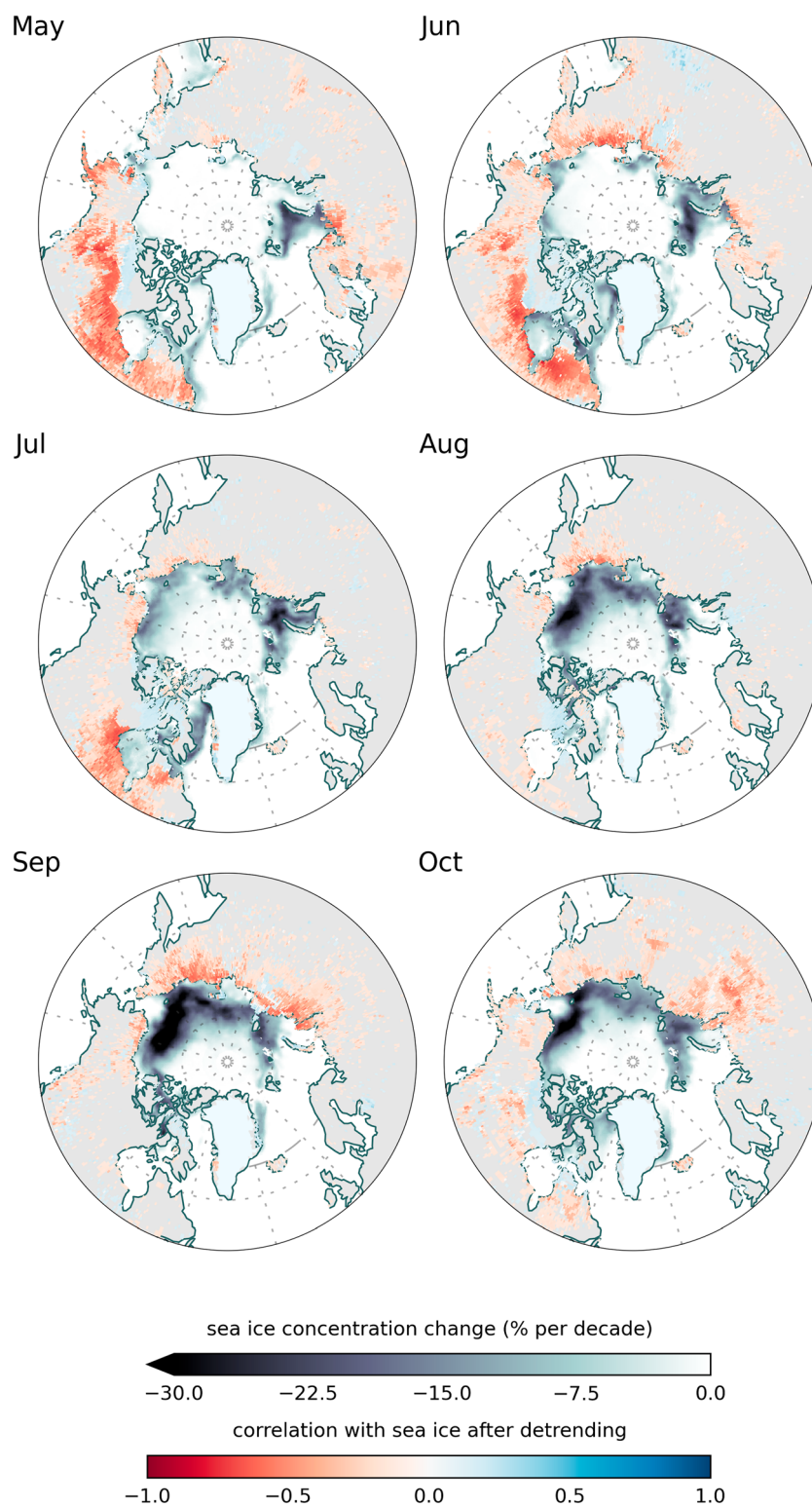
Figure 3. Per month correlations between 1981–2010 terrestrial methane emissions and sea ice concentration. Red to blue colors depict the *r* value of the correlation between modeled methane emissions and sea ice concentration within 2000 km, averaged for all three models. The linear trend in sea ice concentration is shown to indicate areas of high retreat. Note that high correlations do not necessarily equal high emissions.
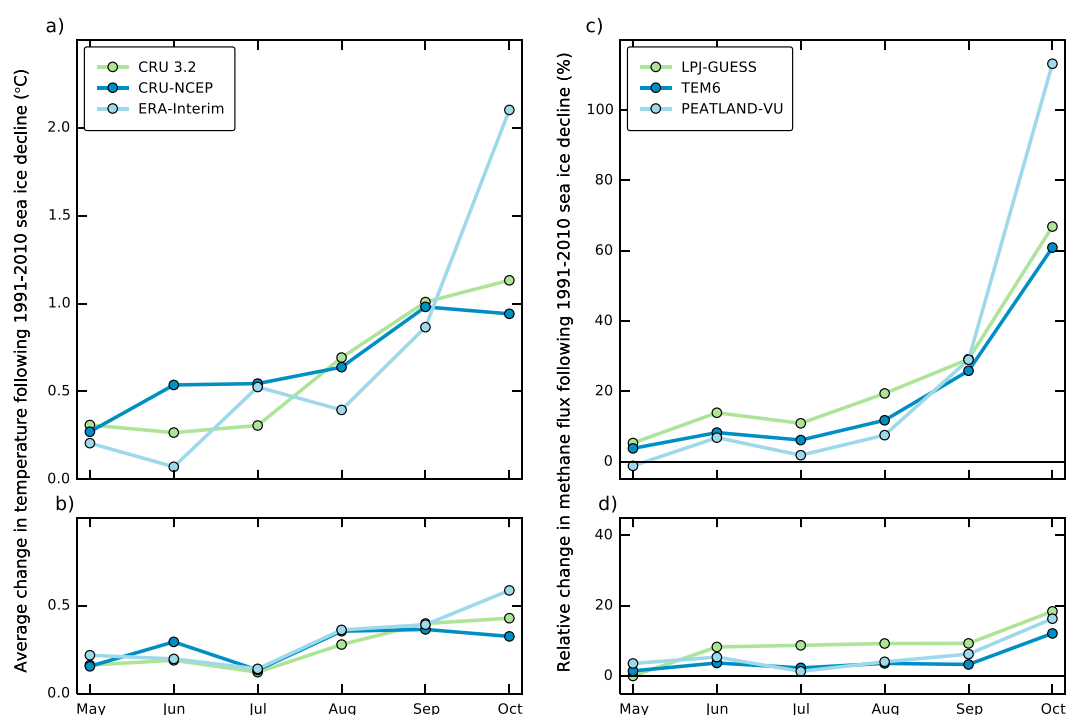
Figure 4. (a and b) Linearly interpolated change in near-surface air temperature and (c and d) modeled methane emissions from northern wetlands following the trend in 1991–2010 sea ice decline, averaged over sea ice-affected (Figures 4a and 4c) and unaffected (Figures 4b and 4d) areas. Temperature change is expressed in °C, while changing methane emissions are expressed as a percentage, both relative to the 1981–1990 average.

(see Figure S4 for details). This suggests that the association between sea ice and methane emissions is strongly temperature driven, rather than through changes in precipitation.

3.2. Relative and Absolute Change in Emissions

Figure 4 shows the increase in temperature and methane emissions for sea ice-affected and unaffected areas. The former is approximately equal to the areas in red in Figure 3, while the latter, where no significant correlations were found, is roughly equal to the grey areas (see Figure S2 for a per model representation). Although Figure 4 shows increasing temperature and methane fluxes for both areas, much stronger trends are observed in sea ice-affected areas. The divergence in trends between the regions is most notable from August to October (see also Figure S5), when the models show a large increase in methane emissions for sea ice-affected areas and temperature increase is highest—although a small increase remains in June.

It is important to note, however, that Figures 4c and 4d show the relative change in emissions. In absolute terms, emissions are highest in midsummer and much lower by the start of autumn, which may limit the impact of sea ice-induced warming. Therefore, the absolute rise in emissions was also determined: by extrapolating the difference in emission trends between the two regions to the observed reductions in sea ice during 2005–2010—the years with lowest sea ice in our study period—we estimate that emissions were on average 1.7 Tg CH_4 yr^{-1} higher in sea ice-affected areas. Per model, the fluxes were 1.5–2.4 Tg CH_4 yr^{-1}, 0.4–0.7 Tg CH_4 yr^{-1}, and 1.8–4.1 Tg CH_4 yr^{-1} higher for LPJ, TEM6, and Peatland-VU, respectively. The upper end of this range is not too distant from a recent atmospheric inversion estimate, which reported an Arctic flux anomaly of 4.4 ± 3.8 Tg CH_4 for 2007 [*Bruhwiler et al.*, 2014]. The lower central estimate presented here can be considered conservative, since the detrending most likely led to an underestimation of the areal extent of the connection with sea ice retreat. Furthermore, the size of these regions in the analysis is kept static from year to year—even though it is likely that the area of influence has expanded given the higher prevalence of sea ice melt in recent years. As sea ice decline continues, its influence on air temperature grows. This may lead to an additional increase in methane emissions on top of what is presented here.

4. Discussion and Conclusions

4.1. Possible Causes Behind Observed Trends

While we have shown that sea ice-associated warming is an important driving force behind recent increases in methane emissions from northern wetlands, it is possible that earlier snowmelt has similarly led to raised temperatures when highly reflective snow gives way to the dark ground beneath. In turn, this warming feedback may lead to higher methane emissions but can also contribute to more sea ice melt—leading to even higher temperatures. This synergy complicates the interpretation of a correlation with sea ice during springtime when both sea ice decline and earlier snowmelt could cause a temperature-related increase in emissions [*Serreze and Barry*, 2011; *Screen et al.*, 2012]. It is, however, important to note that the interannual variation of sea ice in Hudson Bay is largely due to local atmospheric forcing, as there is little export or import of sea ice into the basin and few intrusions of warm water [*Hochheim et al.*, 2011]. It is therefore possible that the close match observed in Figure 3 between sea ice extent and methane emissions in the area surrounding Hudson Bay from May to July is due, in part, to the same external influence that also promotes snowmelt. This may explain the low difference between sea ice-affected and unaffected areas during spring, as shown in Figure 4. Earlier snowmelt may have occurred in both areas, resulting in concomitant higher methane emissions. However, sea ice is undergoing a long-term thinning trend [*Laxon et al.*, 2013] which implies that progressively less warming is needed to melt away the same area of sea ice [*Rind et al.*, 2009], possibly enhancing the importance of the sea ice albedo effect on spring fluxes relative to snowmelt—although this remains difficult to detect at this time.

Spring is also a decisive time for the rest of the sea ice melt season since the area of melt ponds in this period has been shown to be an important predictor of the sea ice minimum [*Schröder et al.*, 2014]. Due to the lower albedo, a higher melt pond area early in the melt season will lead to more absorption of solar radiation, and thus more sea ice melt during the summer. Springtime weather conditions can therefore explain much of the September sea ice extent [*Kapsch et al.*, 2014]. This implies that weather conditions at the end of the melt season are of lesser importance to the state of the sea ice. On the contrary, the strong reduction in autumn sea ice conditions is one of the most important causes behind increased near-surface air temperatures at that time [*Lawrence et al.*, 2008; *Serreze and Barry*, 2011; *Screen et al.*, 2012]. A good match between the interannual variation in sea ice and methane emissions during the later months in Figure 3 is, therefore, unlikely to be due to a similar response from an outside influence but rather a sea ice-related temperature feedback. As a result, the connection between sea ice retreat and higher methane fluxes from terrestrial sources is most easily identified in that time of year.

All three methane models used in this study represent the state of the art in modeling methane emissions from northern wetlands and permafrost regions. Nonetheless, it is important to verify that model agreement is not due to similar assumptions. Surprisingly, however, spatial patterns and emission trends are most dissimilar between TEM6 and Peatland-VU despite sharing some model components as proposed by *Walter and Heimann* [2000]. This may be because of different implementations for both hydrology and net primary production [*Zhuang et al.*, 2004; *Mi et al.*, 2014]. Moreover, the methane subroutine of LPJ-GUESS was developed completely independently [*Wania et al.*, 2010]. Despite these differences among the models, all three show a similar increase in methane emissions toward the autumn, which is likely due to comparable trends in the climate forcing as shown in Figure 4. In general, the models predict that higher temperatures will lead to higher methane emissions, which agrees with observations [*Olefeldt et al.*, 2013]. A more detailed discussion of the similarity and differences between the models is included in the supporting information.

Another strong control on methane emissions is water table depth, since this determines where in the soil production and oxidation of methane take place. Although a strong link between precipitation and sea ice appears absent (see Figure S4), higher temperatures could arguably lead to drier conditions—suppressing methane emissions. However, sea ice retreat has been linked to increasing atmospheric moisture [*Screen and Simmonds*, 2010] and may increase precipitation in the long term [*Bintanja and Selten*, 2014]. This suggests that—in general—sea ice retreat will lead to wetter rather than drier conditions across the Arctic, although large differences may occur regionally [*Watts et al.*, 2014]. We emphasize the continued need to improve methane models and the role of changing hydrology, whether associated to sea ice or not.

4.2. Implications and Conclusions

Sea ice concentrations and terrestrial methane emissions covary throughout vast regions of the Arctic, with the clearest influence of sea ice decline on autumn fluxes, and perhaps to some extent in spring. We estimate that the remote warming influence connected to sea ice decline has, compared to the baseline period of 1981–1990, led to a higher release of 1.7 Tg CH_4 yr^{-1} from the terrestrial Arctic by the years 2005–2010, with an uncertainty range of 0.4–4.1 Tg CH_4 yr^{-1}. Due to constraints imposed on our analysis, such as the detrending of time series and fixed extent of the area influenced by sea ice, we consider this estimate to be modest in size. Since sea ice decline and associated amplified warming on land is expected to persist, a reasonable projection from our results is that methane emissions from northern wetlands will continue to increase [*McGuire et al.*, 2012; *Parmentier et al.*, 2013].

In order to be able to go beyond models and corroborate these connections and trends with flux measurements at the ecosystem level, we need to invest in extending current flux-monitoring programs to cover as much of the year as possible. Most data on methane emissions are collected in summertime [*McGuire et al.*, 2012] when the Arctic is most accessible. If, however, the largest relative changes are expected to occur outside of the summer, those periods should be observed to properly assess long-term trends in emissions and to correctly identify local effects of earlier snowmelt and sea ice retreat. Recent studies that have reported significant emissions far into the autumn [*Sturtevant et al.*, 2012; *Mastepanov et al.*, 2013] underline the importance of observations throughout that season, when connections to sea ice retreat are strongest.

Although extending methane flux measurements to the later part of the year can be logistically, technically, and physically demanding, such actions are necessary to improve our understanding of the effects of sea ice retreat on Arctic greenhouse gas exchange [*Christensen*, 2014], since essential processes may still be underrepresented in the models. Effective complementary application of field measurements and modeling efforts is imperative to verify and predict the ways in which sea ice decline affects Arctic greenhouse gas exchange at distance. The crosscutting nature of such large-scale interactions emphasizes the need for an integrated analysis of the marine and terrestrial carbon cycle within a rapidly changing Arctic.

References

Bhatt, U. S., et al. (2014), Implications of Arctic sea ice decline for the Earth system, *Annu. Rev. Environ. Resour.*, *39*, 57–89, doi:10.1146/annurev-environ-122012-094357.

Bintanja, R., and F. M. Selten (2014), Future increases in Arctic precipitation linked to local evaporation and sea-ice retreat, *Nature*, *509*(7501), 479–482, doi:10.1038/nature13259.

Bruhwiler, L., E. Dlugokencky, K. Masarie, M. Ishizawa, A. Andrews, J. Miller, C. Sweeney, P. Tans, and D. Worthy (2014), CarbonTracker-CH4: An assimilation system for estimating emissions of atmospheric methane, *Atmos. Chem. Phys.*, *14*(16), 8269–8293, doi:10.5194/acp-14-8269-2014.

Christensen, T. R. (2014), Climate science: Understand Arctic methane variability, *Nature*, *509*(7500), 279–281, doi:10.1038/509279a.

Comiso, J. C. (2000), Bootstrap sea ice concentrations from Nimbus-7 SMMR and DMSP SSM/I-SSMIS, Version 2. 1981–2010.

Hayes, D. J., A. D. McGuire, D. W. Kicklighter, K. R. Gurney, T. J. Burnside, and J. M. Melillo (2011), Is the northern high-latitude land-based CO_2 sink weakening?, *Global Biogeochem. Cycles*, *25*, GB3018, doi:10.1029/2010GB003813.

Hochheim, K. P., J. V. Lukovich, and D. G. Barber (2011), Atmospheric forcing of sea ice in Hudson Bay during the spring period, 1980–2005, *J. Mar. Syst.*, *88*(3), 476–487, doi:10.1016/j.jmarsys.2011.05.003.

Kapsch, M.-L., R. G. Graversen, T. Economou, and M. Tjernström (2014), The importance of spring atmospheric conditions for predictions of the Arctic summer sea ice extent, *Geophys. Res. Lett.*, *41*, 5288–5296, doi:10.1002/2014GL060826.

Lawrence, D. M., A. G. Slater, R. A. Tomas, M. M. Holland, and C. Deser (2008), Accelerated Arctic land warming and permafrost degradation during rapid sea ice loss, *Geophys. Res. Lett.*, *35*, L11506, doi:10.1029/2008GL033985.

Laxon, S. W., et al. (2013), CryoSat-2 estimates of Arctic sea ice thickness and volume, *Geophys. Res. Lett.*, *40*, 732–737, doi:10.1002/grl.50193.

Mastepanov, M., C. Sigsgaard, T. Tagesson, L. Strom, M. P. Tamstorf, M. Lund, and T. R. Christensen (2013), Revisiting factors controlling methane emissions from high-Arctic tundra, *Biogeosciences*, *10*(7), 5139–5158, doi:10.5194/bg-10-5139-2013.

McGuire, A. D., et al. (2010), An analysis of the carbon balance of the Arctic Basin from 1997 to 2006, *Tellus B*, *62*(5), 455–474, doi:10.1111/j.1600-0889.2010.00497.x.

McGuire, A. D., et al. (2012), An assessment of the carbon balance of arctic tundra: Comparisons among observations, process models, and atmospheric inversions, *Biogeosciences*, *9*(8), 3185–3204, doi:10.5194/bg-9-3185-2012.

Melton, J. R., et al. (2013), Present state of global wetland extent and wetland methane modelling: Conclusions from a model inter-comparison project (WETCHIMP), *Biogeosciences*, *10*, 753–788, doi:10.5194/bg-10-753-2013.

Mi, Y., J. van Huissteden, F. J. W. Parmentier, A. Gallagher, A. Budishchev, C. T. Berridge, and A. J. Dolman (2014), Improving a plot-scale methane emission model and its performance at a northeastern Siberian tundra site, *Biogeosciences*, *11*(14), 3985–3999, doi:10.5194/bg-11-3985-2014.

Najafi, M. R., F. W. Zwiers, and N. P. Gillett (2015), Attribution of Arctic temperature change to greenhouse-gas and aerosol influences, *Nat. Clim. Change*, *5*(3), 246–249, doi:10.1038/nclimate2524.

Olefeldt, D., M. R. Turetsky, P. M. Crill, and A. D. McGuire (2013), Environmental and physical controls on northern terrestrial methane emissions across permafrost zones, *Global Change Biol.*, *19*(2), 589–603, doi:10.1111/gcb.12071.

Parmentier, F. J. W., T. R. Christensen, L. L. Sørensen, S. Rysgaard, A. D. McGuire, P. A. Miller, and D. A. Walker (2013), The impact of lower sea-ice extent on Arctic greenhouse-gas exchange, *Nat. Clim. Change*, *3*, 195–202, doi:10.1038/nclimate1784.

Petrescu, A. M. R., L. P. H. van Beek, J. van Huissteden, C. Prigent, T. Sachs, C. A. R. Corradi, F. J. W. Parmentier, and A. J. Dolman (2010), Modeling regional to global CH$_4$ emissions of boreal and arctic wetlands, *Global Biogeochem. Cycles*, 24, GB4009, doi:10.1029/2009GB003610.

Pistone, K., I. Eisenman, and V. Ramanathan (2014), Observational determination of albedo decrease caused by vanishing Arctic sea ice, *Proc. Natl. Acad. Sci. U.S.A.*, 111(9), 3322–3326, doi:10.1073/pnas.1318201111.

Rind, D., R. Healy, C. Parkinson, and D. Martinson (2009), The role of sea ice in 2×CO$_2$ climate model sensitivity: Part I. The total influence of sea ice thickness and extent, *J. Clim.*, 8(3), 449–463, doi:10.1175/1520-0442(1995)008<0449:TROSII>2.0.CO;2.

Schröder, D., D. L. Feltham, D. Flocco, and M. Tsamados (2014), September Arctic sea-ice minimum predicted by spring melt-pond fraction, *Nat. Clim. Change*, 4, 353–357.

Screen, J. A., and I. Simmonds (2010), The central role of diminishing sea ice in recent Arctic temperature amplification, *Nature*, 464(7293), 1334–1337, doi:10.1038/nature09051.

Screen, J. A., C. Deser, and I. Simmonds (2012), Local and remote controls on observed Arctic warming, *Geophys. Res. Lett.*, 39, L10709, doi:10.1029/2012GL051598.

Serreze, M. C., and R. G. Barry (2011), Processes and impacts of Arctic amplification: A research synthesis, *Global Planet. Change*, 77, 85–96, doi:10.1016/j.gloplacha.2011.03.004.

Smith, B., I. C. Prentice, and M. T. Sykes (2001), Representation of vegetation dynamics in the modelling of terrestrial ecosystems: Comparing two contrasting approaches within European climate space, *Global Ecol. Biogeogr.*, 10(6), 621–637.

Sturtevant, C. S., W. C. Oechel, D. Zona, Y. Kim, and C. E. Emerson (2012), Soil moisture control over autumn season methane flux, Arctic Coastal Plain of Alaska, *Biogeosciences*, 9, 1423–1440, doi:10.5194/bg-9-1423-2012.

van Huissteden, J., R. van den Bos, and I. M. Alvarez (2006), Modelling the effect of water-table management on CO$_2$ and CH$_4$ fluxes from peat soils, *Neth. J. Geosci.*, 85(1), 3–18.

Walter, B. P., and M. Heimann (2000), A process-based, climate-sensitive model to derive methane emissions from natural wetlands: Application to five wetland sites, sensitivity to model parameters, and climate, *Global Biogeochem. Cycles*, 14(3), 745–765.

Wania, R., I. Ross, and I. C. Prentice (2010), Implementation and evaluation of a new methane model within a dynamic global vegetation model: LPJ-WHyMe v1.3.1, *Geosci. Model Dev.*, 3(2), 565–584, doi:10.5194/gmd-3-565-2010.

Watts, J. D., J. S. Kimball, A. Bartsch, and K. C. McDonald (2014), Surface water inundation in the boreal-Arctic: Potential impacts on regional methane emissions, *Environ. Res. Lett.*, 9(7), 075001, doi:10.1088/1748-9326/9/7/075001.

Zhuang, Q., J. M. Melillo, D. W. Kicklighter, R. G. Prinn, A. D. McGuire, P. A. Steudler, B. S. Felzer, and S. Hu (2004), Methane fluxes between terrestrial ecosystems and the atmosphere at northern high latitudes during the past century: A retrospective analysis with a process-based biogeochemistry model, *Global Biogeochem. Cycles*, 18, GB3010, doi:10.1029/2004GB002239.